

## 266. An ESR. and ENDOR. Study of the Radical Anions of Cyano- and Nitro-Monosubstituted Naphthalenes

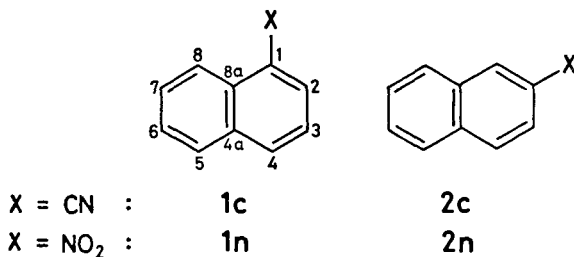
by **Peter Fürderer** and **Fabian Gerson**

Physikalisch-Chemisches Institut der Universität Basel, CH-4056 Basel, Klingelbergstrasse 80

(8. IX. 76)

*Summary.*  $^1\text{H}$ - and  $^{14}\text{N}$ -coupling constants have been determined by ESR. and ENDOR. spectroscopy for the radical anions of 1- and 2-cyano-, and 1- and 2-nitronaphthalene.

To our knowledge, no hyperfine data have yet been reported for the radical anions of such simple  $\pi$ -systems as naphthalenes monosubstituted by cyano and nitro groups, presumably because of the relative complexity of their ESR. spectra which makes reliable analysis rather difficult. A brief communication on these spectra seems therefore appropriate, the more so as the acquisition of the pertinent data provides a further example of an application of the ENDOR. method to radicals of low symmetry [1].



**Results.** – The radical anions of 1- and 2-cyano- (**1c** resp. **2c**), and of 1- and 2-nitronaphthalene (**1n** resp. **2n**) were prepared from the corresponding neutral compounds both by reaction with potassium in 1,2-dimethoxyethane (DME) and by electrolytic reduction in N,N-dimethylformamide (DMF) with tetraethylammonium perchlorate as the supporting salt. For technical reasons, ENDOR. studies could be performed only on the radical anions produced by the former, ‘chemical’ method. In such studies (DME/ $\text{K}^\oplus$  as the solvent/counterion), a temperature of  $-90^\circ$  proved to be the most convenient for an optimal ENDOR. enhancement [2]. It is noteworthy that the proton ENDOR. signals of the nitro substituted radical anions were broader than those in the spectra of the cyano analogues, the widths at the half-heights being *ca.* 0.15, 0.20, 0.30 and 0.30 MHz for **1c**  $\cdot^\ominus$ , **2c**  $\cdot^\ominus$ , **1n**  $\cdot^\ominus$  and **2n**  $\cdot^\ominus$ , respectively. This behaviour reflected to a certain degree the strikingly different appearance of the ESR. spectra taken under the same conditions. Whereas the hyperfine patterns of **1c**  $\cdot^\ominus$  and **2c**  $\cdot^\ominus$  were highly resolved (peak-to-peak widths of 0.06 resp. 0.07 Gauss<sup>1)</sup>)

1) 1 Gauss =  $10^{-4}$  Tesla.

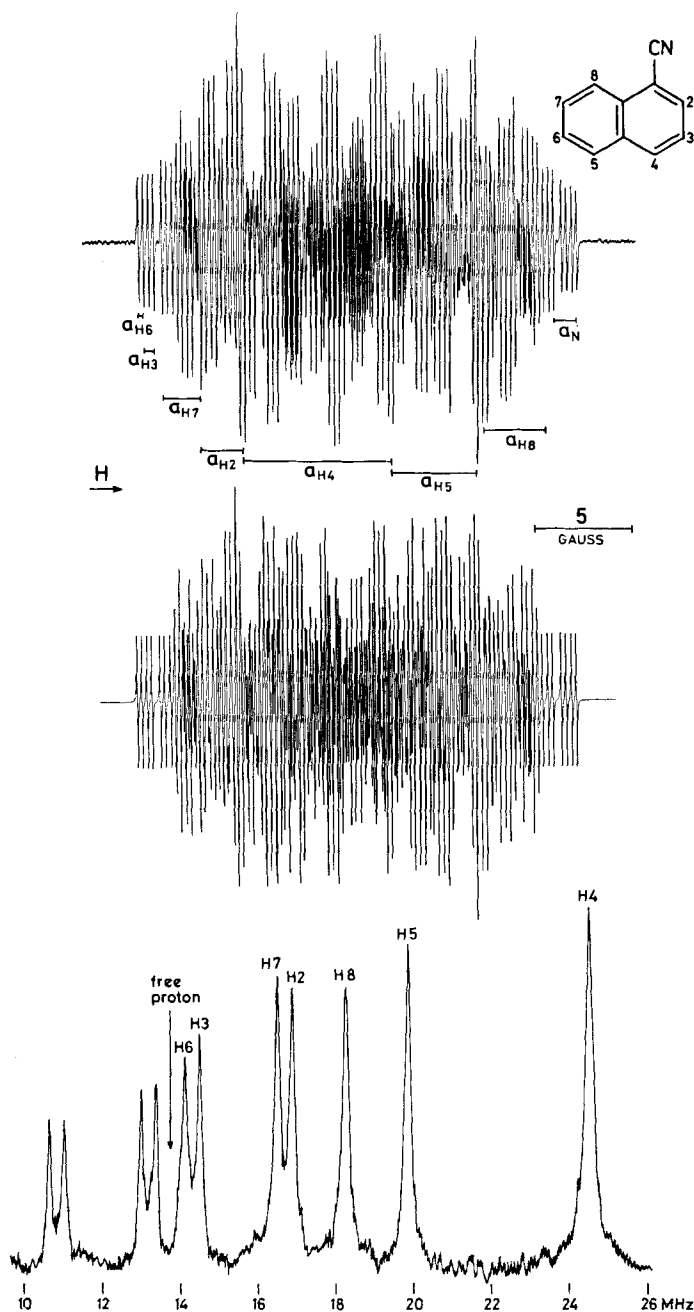


Fig. 1. ESR. and ENDOR. spectra of the radical anion  $1c \cdot^-$ . Top: ESR. spectrum. Solvent: DME; counterion:  $K^+$ ; temp.:  $-90^\circ$ . Bottom: ENDOR. spectrum taken under the same conditions. Middle: Computer simulated ESR. spectrum. Coupling constants as given in the Table; line-shape: Lorentzian; line-width: 0.06 Gauss.

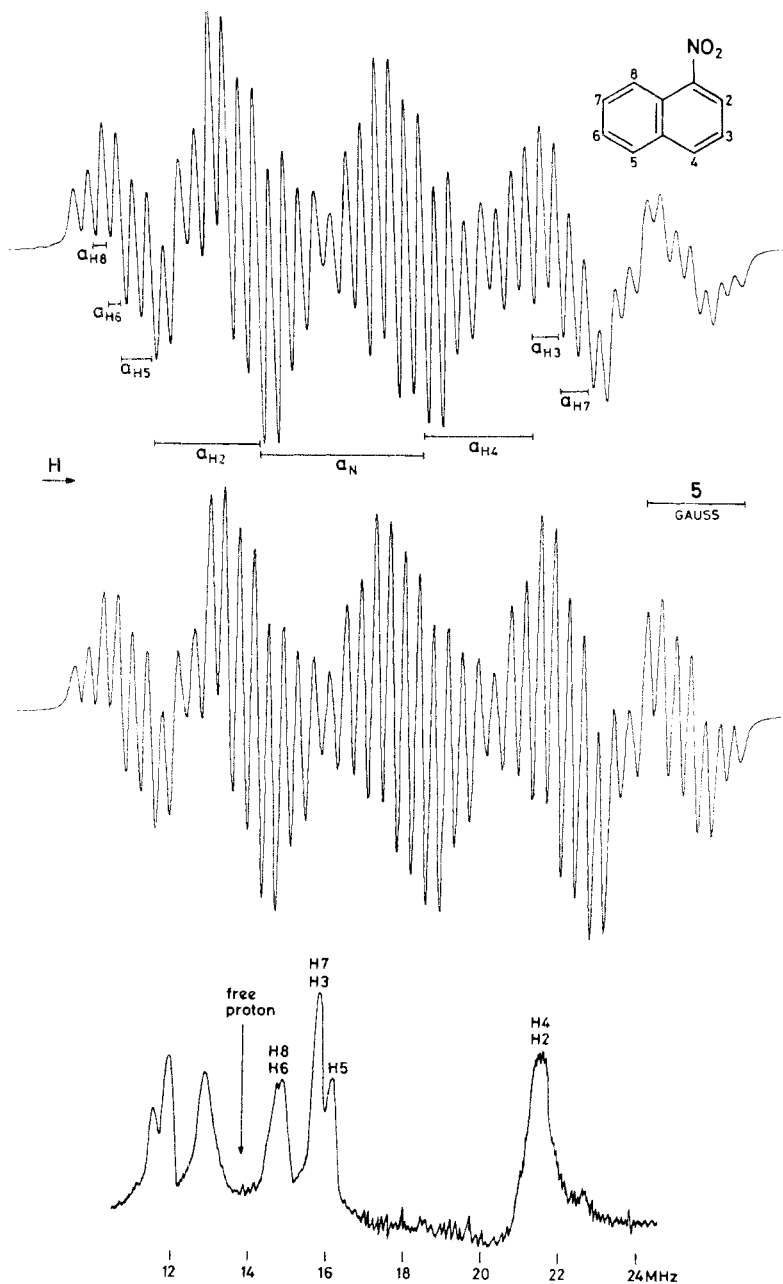


Fig. 2. ESR. and ENDOR. spectra of the radical anion  $1n \cdot ^-$ . Top: ESR. spectrum. Solvent: DME; counterion:  $K^+$ ; temp.:  $-90^\circ$ . Bottom: ENDOR. spectrum taken under the same conditions. Middle: Computer simulated ESR. spectrum. Coupling constants as given in the Table; line-shape: Lorentzian; line-width: 0.50 Gauss. The simulation does not allow for the *specific* broadening (due to the effects of  $g$  and  $^{14}N$  anisotropies), in particular for the larger line-width at the high-field as compared to the low-field side of the spectrum.

those of  $\mathbf{1n} \cdot \ominus$  and  $\mathbf{2n} \cdot \ominus$  consisted of broad components (widths of 0.50 resp. 0.40 Gauss<sup>2)</sup>). An illustration of this difference is provided by Fig. 1 and 2 which show the ESR. and ENDOR. spectra observed at  $-90^\circ$  for the chemically produced radical anions  $\mathbf{1c} \cdot \ominus$  and  $\mathbf{1n} \cdot \ominus$ .

Moderately good, and in all cases comparable resolution (peak-to-peak widths of 0.08 Gauss for  $\mathbf{1c} \cdot \ominus$  and  $\mathbf{2c} \cdot \ominus$ , and of 0.10 Gauss for  $\mathbf{1n} \cdot \ominus$  and  $\mathbf{2n} \cdot \ominus$ ) was exhibited by the ESR. spectra taken at the ambient temperature ( $+25^\circ$ ) of the electrolytically generated radical anions (DMF/Et<sub>4</sub>N<sup>⊕</sup> as the solvent/counterion).

The procedure adopted in the analysis of the hyperfine structures of  $\mathbf{1c} \cdot \ominus$ ,  $\mathbf{2c} \cdot \ominus$ ,  $\mathbf{1n} \cdot \ominus$  and  $\mathbf{2n} \cdot \ominus$  was as follows:

1. The coupling constants,  $a_{\text{H}\mu}$ , of the seven non-equivalent protons in each of the four radical anions were derived from the positions of the ENDOR. signals. For  $\mathbf{1c} \cdot \ominus$ , all protons displayed well separated absorptions (Fig. 1) so that a mere inspection of the ENDOR. spectrum yielded the required data. In other cases, where some of the signals coincided (see Fig. 2 for  $\mathbf{1n} \cdot \ominus$ ), the number of protons involved had to be determined by a careful examination of the corresponding ESR. spectra, since the ENDOR. intensities alone are not a reliable guide in this respect [1] [3].

2. Together with the additional <sup>14</sup>N-coupling constant ( $a_{\text{N}}$ ), which was readily obtained from each ESR. spectrum, the  $a_{\text{H}\mu}$  values afforded by the ENDOR. studies served for computer simulation of the ESR. hyperfine patterns found under the same conditions (solvent/counterion: DME/K<sup>⊕</sup>; temp.:  $-90^\circ$ ). These values were employed in a straightforward way for protons giving rise to separate ENDOR. signals (see above), while, in the cases of an accidental coincidence of such signals, the apparent equivalence of the protons was removed by adopting slightly differing coupling constants  $a_{\text{H}\mu}$ . The agreement achieved in the simulation is demonstrated in Fig. 1 and 2 where the derivative curves computed for  $\mathbf{1c} \cdot \ominus$  and  $\mathbf{1n} \cdot \ominus$  are reproduced below the respective ESR. spectra.

3. The hyperfine data,  $a_{\text{H}\mu}$  and  $a_{\text{N}}$ , thus established for the chemically prepared radical anions were subsequently used as starting parameters in the unravelling of the ESR. splitting patterns for their electrolytically generated analogues (solvent/counterion: DMF/Et<sub>4</sub>N<sup>⊕</sup>; temp.:  $+25^\circ$ ). Systematic variation of these values gave in all cases an excellent fit to the spectra by means of computer simulated derivative curves.

The proton and <sup>14</sup>N-coupling constants ( $a_{\text{H}\mu}$  and  $a_{\text{N}}$ ) for the four radical anions and both choices of experimental conditions (solvent/counterion and temperature) are listed in the Table. The assignment of the  $a_{\text{H}\mu}$  values to the seven protons in the non-equivalent positions  $\mu$  will be justified later in this paper.

**Discussion.** – *Line-widths.* The conspicuous broadening observed at  $-90^\circ$  in the ESR. spectra of the nitro substituted radical anions  $\mathbf{1n} \cdot \ominus$  and  $\mathbf{2n} \cdot \ominus$  with DME/K<sup>⊕</sup> as the solvent/counterion is certainly due to the effect of  $g$  and <sup>14</sup>N hyperfine anisotropies combined with that of ion pairing (through unresolved splitting from the <sup>39</sup>K nucleus of the cation). Under these conditions, large line-widths are usually found for radical anions such as  $\mathbf{1n} \cdot \ominus$  and  $\mathbf{2n} \cdot \ominus$  in which the nitro substituent accommodates a considerable portion of the  $\pi$ -spin population [4]. The narrower lines displayed by the ESR. spectra of  $\mathbf{1n} \cdot \ominus$  and  $\mathbf{2n} \cdot \ominus$  taken at  $+25^\circ$  with DME/Et<sub>4</sub>N<sup>⊕</sup> as the solvent/counterion are also conforming to the previous experience (see *e.g.* [5]), since the effects of anisotropies and ion pairing are alleviated at higher temperature and in

<sup>2)</sup> Measured at the low-field side of the spectra.

polar solvents, respectively. The factors which affect the resolution of the ESR hyperfine components for the two radical anions are thus rather well understood. A problem deserving further systematic studies is the extent to which the effects considered above also contribute to the increased width of the ENDOR signals observed for  $1n \cdot \ominus$  and  $2n \cdot \ominus$  under the same conditions as the broadening of the ESR lines.

*Assignment of the proton coupling constants.* Since the  $a_{H\mu}$  values for the radical anions  $1c \cdot \ominus$ ,  $2c \cdot \ominus$ ,  $1n \cdot \ominus$  and  $2n \cdot \ominus$  are not strongly altered by a change in the experimental conditions (Table<sup>3</sup>), their discussion will be restricted to the data acquired at  $-90^\circ$  with DME/ $K^{\oplus}$  as the solvent/counterion. For an assignment of these data, it is tempting to recur to some qualitative arguments, prior to the use of more quantitative methods, such as the calculations of  $\pi$ -spin populations  $\rho_\mu$  by

Table.  $^1H$ - and  $^{14}N$ -coupling constants (in Gauss =  $10^{-4}$  Tesla) for the radical anions of cyano- and nitro-monosubstituted naphthalenes

Radical anion Substituent	DME/ $K^{\oplus}$ ; $-90^\circ C$				DMF/ $Et_4N^{\oplus}$ ; $+25^\circ C$				
	$1c \cdot \ominus$	$2c \cdot \ominus$	$1n \cdot \ominus$	$2n \cdot \ominus$	$1c \cdot \ominus$	$2c \cdot \ominus$	$1n \cdot \ominus$	$2n \cdot \ominus$	
	1-CN	2-CN	1-NO <sub>2</sub>	2-NO <sub>2</sub>	1-CN	2-CN	1-NO <sub>2</sub>	2-NO <sub>2</sub>	
$a_{H\mu}$	$\mu=1$	-	6.92	-	5.49	-	6.94	-	5.52
	2	2.22	-	5.47	-	2.27	-	5.44	-
	3	0.53 <sup>a)</sup>	0.55	1.41	1.58	0.42 <sup>a)</sup>	0.58	1.37	1.51
	4	7.66	4.34	5.58	0.74 <sup>a)</sup>	7.85	4.35	5.52	0.78 <sup>a)</sup>
	5	4.38	3.57	1.62	0.72 <sup>a)</sup>	4.65	3.46	1.65	0.69 <sup>a)</sup>
	6	0.26 <sup>a)</sup>	1.50	0.65 <sup>a)</sup>	1.79	<0.08 <sup>a)</sup>	1.34	0.62 <sup>a)</sup>	1.70
	7	1.95	0.51	1.46	0.91 <sup>a)</sup>	1.70	0.56	1.41	0.78 <sup>a)</sup>
	8	3.20	4.54	0.75 <sup>a)</sup>	2.28	3.08	4.45	0.70 <sup>a)</sup>	2.21
$a_N$	1.20	1.29	8.45	9.33	1.28	1.30	7.72	8.53	
error	$\pm 0.01$	$\pm 0.02$	$\pm 0.05$	$\pm 0.05$	$\pm 0.02$	$\pm 0.02$	$\pm 0.03$	$\pm 0.03$	

a) Assignment uncertain.

means of standard MO models. Two approaches suggest themselves. The first one is applicable only to the cyano derivatives  $1c \cdot \ominus$  and  $2c \cdot \ominus$  in which the substituent effect is not as pronounced as in their nitro counterparts  $1n \cdot \ominus$  and  $2n \cdot \ominus$ . By analogy to the proton coupling constants for the radical anion of naphthalene ( $a_{H1,4,5,8} = 4.95$  Gauss  $\gg a_{H2,3,6,7} = 1.85$  Gauss), those for  $1c \cdot \ominus$  and  $2c \cdot \ominus$  can be divided into two sets. In the case of  $1c \cdot \ominus$ , the first set ( $\mu = 4, 5, 8$ ) comprises the three larger  $a_{H\mu}$  values of 7.66, 4.38 and 3.20 Gauss, whilst the second ( $\mu = 2, 3, 6, 7$ ) consists of the

<sup>3)</sup> Such alterations are even less in the case of  $1n \cdot \ominus$  and  $2n \cdot \ominus$  than in that of  $1c \cdot \ominus$  and  $2c \cdot \ominus$ . The pronounced decrease in the  $^{14}N$ -coupling constants found for the two former radical anions on going from DME/ $K^{\oplus}$  at  $-90^\circ$  to DMF/ $Et_4N^{\oplus}$  at  $+25^\circ$  is presumably caused by a  $\pi$ -spin redistribution within the nitro group itself rather than by a shift of spin population from the substituent into the naphthalene  $\pi$ -system.

four remaining ones. The corresponding sets for  $2c \cdot \ominus$  are formed by the four coupling constants  $a_{H\mu}$  of 6.92, 4.54, 4.34 and 3.57 Gauss ( $\mu = 1, 4, 5, 8$ ), on one hand, and by the three residual values ( $\mu = 3, 6, 7$ ), on the other.

The second approach makes use of mesomeric structures ( $M\mu$ ) in which the negative charge is localized on the substituent (X) and the odd electron is distributed over the carbon centres ( $\mu$ ) of the naphthalene  $\pi$ -system. According to this simple picture, presented in Fig. 3, the radical anions such as  $1c \cdot \ominus$  and  $1n \cdot \ominus$ , which are substituted

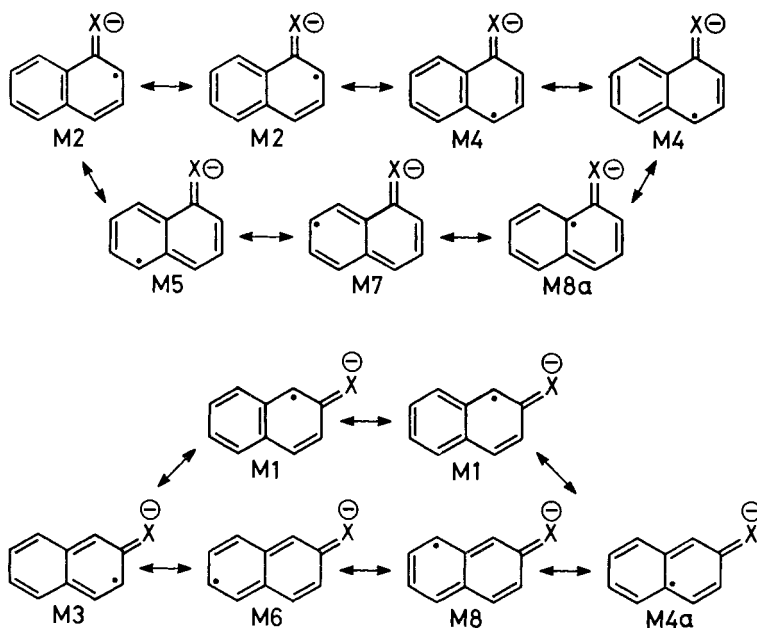


Fig. 3. Mesomeric structures  $M\mu$  for the radical anions of naphthalene substituted by an electron withdrawing group X (cf. text).

in the 1-position by an electron withdrawing group X, should exhibit appreciable  $\pi$ -spin populations  $\rho_\mu$  at the centres  $\mu = 2, 4, 5, 7$  and 8a. Moreover, the ratios of the  $\rho_\mu$  values at the proton bearing centers  $\mu$  and of the coupling constants  $a_{H\mu}$  are predicted to be  $\rho_2:\rho_4:\rho_5:\rho_7 = a_{H2}:a_{H4}:a_{H5}:a_{H7} = 2^2:2^2:1^2:1^2$ . Analogously, for the radical anions such as  $2c \cdot \ominus$  and  $2n \cdot \ominus$  with the substituent X in the 2-position, essential  $\pi$ -spin populations  $\rho_\mu$  should occur at the centres  $\mu = 1, 3, 6, 8$  and 4a, whereby the expected ratios are  $\rho_1:\rho_3:\rho_6:\rho_8 = a_{H1}:a_{H3}:a_{H6}:a_{H8} = 2^2:1^2:1^2:1^2$ .

The mesomeric structures  $M\mu$  work surprisingly well in the case of the nitro substituted radical anions  $1n \cdot \ominus$  and  $2n \cdot \ominus$ . As predicted by these structures, *two* large proton coupling constants of 5.58 and 5.47 Gauss were found for  $1n \cdot \ominus$ ; they are easily identified with  $a_{H2} \approx a_{H4}$ . Two out of the three next largest  $a_{H\mu}$  values of 1.62, 1.46 and 1.41 Gauss, which are by a factor 3.5 to 4.0 smaller than  $a_{H2}$  and  $a_{H4}$ , can consequently be assigned to  $\mu = 5, 7$ , whereas the third one, not accounted for by the structures  $M\mu$ , certainly arises from a substantial negative  $\pi$ -spin population  $\rho_3$  at

the centre  $\mu = 3$ . (Such a population is brought about by the high positive  $\pi$ -spin populations  $\rho_2$  and  $\rho_4$  at the neighbouring centres 2 and 4 via the  $\pi$ - $\pi$  spin polarization mechanism.) Also in accord with the prediction of the structures  $M\mu$  is the occurrence for  $2\mathbf{n} \cdot \ominus$  of a *single* large proton coupling constant of 5.49 Gauss; its identification with  $a_{H1}$  is obvious. The subsequent, three middle-sized  $a_{H\mu}$  values of 2.28, 1.79 and 1.58 Gauss are here readily assigned to  $\mu = 3, 6, 8$ .

The weight of the mesomeric structures  $M\mu$  is considerably less in the case of the cyano substituted radical anions than in that of their nitro counterparts. Nevertheless, these structures may be used to refine the overall assignment made previously for  $1\mathbf{c} \cdot \ominus$  and  $2\mathbf{c} \cdot \ominus$  by analogy with the data for the radical anion of naphthalene. Thus, within the set of the larger  $a_{H\mu}$  values for  $1\mathbf{c} \cdot \ominus$  ( $\mu = 4, 5, 8$ ), the coupling constant of 7.66 Gauss can be identified with  $a_{H4}$ , since the latter should notably exceed  $a_{H5}$  and  $a_{H8}$  in magnitude. Likewise, in view of the inequality  $a_{H2} > a_{H7} > a_{H3}, a_{H6}$ , expected within the second set of the remaining  $a_{H\mu}$  values ( $\mu = 2, 3, 6, 7$ ), the coupling constants of 2.22 and 1.95 Gauss are now assigned to  $\mu = 2$  and 7, respectively. In the case of  $2\mathbf{c} \cdot \ominus$ , the structures  $M\mu$  lead to the relationships  $a_{H1} > a_{H8} > a_{H4}, a_{H5}$  and  $a_{H3}, a_{H6} > a_{H7}$  within the two corresponding sets ( $\mu = 1, 4, 5, 8$  and  $\mu = 3, 6, 7$ ). These relationships require that the largest  $a_{H\mu}$  values of 6.92 and 4.54 Gauss should be assigned to  $\mu = 1$  and 8, respectively, whereas the smallest one (0.51 Gauss) has to be identified with  $a_{H7}$ .

The assignments of the proton coupling constants, as suggested by the arguments presented above, were confirmed and completed by correlating the  $a_{H\mu}$  values with the  $\pi$ -spin populations  $\rho_\mu$  computed by the procedure of *McLachlan* [6]. These calculations utilized the HMO parameters proposed by *Rieger & Fraenkel* for the cyano [7] and nitro substituted [5] radical anions (CN group:  $\alpha_N = \alpha + \beta$ ;  $\beta_{C \equiv N} = 2\beta$  and  $\beta_{C-N} = 0.9\beta$ . NO<sub>2</sub> group:  $\alpha_N = \alpha + 2.2\beta$ ;  $\alpha_O = \alpha + 1.4\beta$ ;  $\beta_{N=O} = 1.67\beta$  and  $\beta_{C-N} = 1.2\beta$ ). With the exception of a few cases involving the smallest  $a_{H\mu}$  values (Table), all coupling constants could be reliably assigned to the protons in the individual positions  $\mu$ .

This work was supported by the *Schweizerischer Nationalfonds zur Förderung der wissenschaftlichen Forschung* (Project Nr. 2.313.75). Financial assistance by *Ciba-Geigy SA, Sandoz SA* and *F. Hoffmann-La Roche & Cie. SA* is also acknowledged.

## REFERENCES

- [1] See, e.g., *F. Gerson, J. Jachimowicz, K. Möbius, R. Biehl, J. S. Hyde & D. S. Leniart*, *J. magn. Res.* **18**, 471 (1975); *Ch. Wydler*, Thesis, University of Basel 1976.
- [2] *F. Gerson, W. B. Maytin, Jr., & Ch. Wydler*, *J. Amer. chem. Soc.* **98**, 1318 (1976); *F. Gerson, K. Müllen & Ch. Wydler*, *Helv.* **59**, 1371 (1976).
- [3] *N. M. Atherton*, 'Electron Spin Resonance', *J. Wiley and Sons*, New York 1973, Chapter 10.
- [4] *R. L. Ward*, *J. chem. Physics* **28**, 518 (1958); *J. Amer. chem. Soc.* **83**, 1296 (1961).
- [5] *P. H. Rieger & G. K. Fraenkel*, *J. chem. Physics* **39**, 609 (1963).
- [6] *A. D. McLachlan*, *Mol. Physics* **3**, 233 (1960).
- [7] *P. H. Rieger & G. K. Fraenkel*, *J. chem. Physics* **37**, 2795 (1962).